Dynamic Interference-Avoiding MIMO Links

Sanaz Naderi*, Dimitris A. Pados*, George Sklivanitis*, Elizabeth Serena Bentley[†],

Joseph Suprenant[†], and Michael J. Medley[†]

*Center for Connected Autonomy and AI, Florida Atlantic University, Boca Raton, FL 33431 USA

[†]Air Force Research Laboratory, Rome, NY 13440, USA

*E-mail: {snaderi2021, dpados, gsklivanitis}@fau.edu

[†]E-mail: {elizabeth.bentley.3, joseph.suprenant, michael.medley}@us.af.mil

Abstract—We address the problem of dynamically optimizing arbitrary multiple-input multiple-output (MIMO) wireless links that may or may not be directional to avoid interference over a fixed frequency band. The optimization is, therefore, applicable to near-field machine-to-machine communications. Specifically, we aim to determine the transmitter beam weight vector and pulse code sequence that maximize the signal-to-interferenceplus-noise ratio (SINR) at the output of the joint maximum-SINR space-time receiver filter. We propose a novel and simple model-based solution that we call space-first-time-next waveform optimization where we optimize first the transmit weight vector (space) and then the pulse code sequence (time). We derive the solution formally and evaluate its performance through extensive simulation studies considering varying waveform code length, near-field/far-field conditions, and spread-spectrum/non-spreadspectrum interference. The studies demonstrate the effectiveness of the proposed method and its remarkable interference avoidance capability in dense interference scenarios compared to static conventionally designed MIMO links.

Index Terms—Autonomous communications, directional networking, interference avoidance, jam resistant communications, MIMO, near field communications, space-time waveform design.

I. INTRODUCTION

Throughout the evolution of wireless communication systems, electromagnetic interference has always been a vital consideration [1]. The exponential rise in the number of wireless users, the expectation of data transfer rates in the order of hundreds of Mbps, and emerging technologies such as machine-to-machine communications, mm-wave robotics, wireless security [2]–[4], and more, make managing and preventing interference increasingly difficult [1], [5], [6].

An effective approach to address interference concerns is through interference avoidance utilizing dynamic waveform design at a fine time scale [7]–[9] where a finite sequence of repeated pulses (such as square-root-raised cosines (SRRC)) that span the entire continuum of the device-accessible spectrum is code optimized over a finite pulse-modulation alphabet to maximize the signal-to-interference-plus-noise ratio (SINR) at the output of the max-SINR filter at the intended receiving node [10], [11].

This work was supported in part by the National Science Foundation under Grants CNS-2027138, CNS-2117822 and EEC-2133516 and the Air Force Research Laboratory under Grant FA8750-21-1-0500. Distribution A. Approved for public release: Distribution unlimited: AFRL-2023-3173 on 30 June 2023.

Multiple-input multiple-output (MIMO) technology has emerged as a critical element in modern communications, both in the context of 5G and future generations [12]–[14] and mesh networking. The significance of MIMO systems lies in their ability to enhance channel capacity or minimize bit-error-rate (BER) and optimize power consumption while maintaining a fixed channel data rate. Moreover, MIMO systems offer distinctive advantages for interference management through the utilization of directional transmission, space-time precoding, directional reception, and space-time filtering. These techniques effectively leverage the combined potential of spatial and time domain degrees of freedom (DOF) [15] leading to superior performance and improved overall system efficiency.

There is significant active research in the field to address interference challenges in the time domain. One approach involves the utilization of distributed deep learning models, as demonstrated in [16], which specifically focuses on 5G/broadband IoT networks. In [11], an alternative solution is considered for an IoT network where rather than employing deep learning, the authors propose an optimal adaptive sparse waveform design algorithm. The algorithm digitally adjusts the waveform shape to maximize the SINR at the output of the receiver's maximum-SINR linear filter. Furthermore, the work in [10] addresses the opportunity for directional space-time waveform design in narrowband far-field MIMO systems to avoid proactively interference. The authors propose a solution that involves optimizing both the pulse code sequence and the signal angle-of-arrival (AoA) to establish communication between the intended transmitter and receiver pair. The optimization maximizes the maximum achievable pre-detection SINR at the output of the max-SINR receiver filter.

In this paper, we present a solution to the challenge of establishing an optimally interference-avoiding near-field or far-field MIMO wireless link targeting modern connected robotics applications in high frequency bands (i.e., mm-wave or THz) where near-field effects may be significantly extended when the diameter of focused antennas exceeds half the wavelength of the carrier or as the carrier wavelength decreases. Specifically, we investigate the optimization of the transmitter beam weight vector and the time-domain wave shaping code to maximize the pre-detection SINR at the output of the joint space-time receiver filter for any locally sensed space-time

disturbance autocorrelation matrix. Our solution presents a novel model-based approach to overcome the limitations of conventional directional array-response modeling in near-field MIMO wireless links. Firstly, we optimize the transmitter beam weight vector and then we shape a digitally coded waveform that utilizes the entire device accessible frequency band. Our contributions can be summarized as follows:

- We present a new closed-loop design of transmit spacetime signals to dynamically maximize the SINR at the output of the receiver's space-time matched filter for any locally sensed space-time disturbance autocorrelation matrix. This involves a two-step process: Searching for an optimized transmitter beam weight vector first and subsequently optimizing a digital wave shape code.
- The proposed method is thoroughly evaluated and compared through extensive simulations in diverse interference scenarios. The types of interference scenarios include near-field and far-field, spread-spectrum and nonspread-spectrum, as well as light and dense disturbance scenarios. The simulation studies investigate the impact of varying transmit beam vector and waveform code lengths. The results demonstrate how the potential scheme can effectively support near/far-field MIMO links in extremely challenging interference environments.

Notation: Matrices are denoted by upper-case bold letters, column vectors by lower-case bold letters, and scalars by lower-case plain-font letters. The transpose operation is represented by the superscript T , the Hermitian operation (conjugate transpose) by H , and the Kronecker product by \otimes .

II. MIMO SYSTEM MODEL

In Fig. 1, we consider a MIMO link configuration with M_t transmit and M_r receive antennas and without loss of generality we assume that the transmitter sends an information bit sequence $b(n) \in \{\pm 1\}$, n = 0, 1, ..., N, at rate $1/T_b$ across all antennas on a carrier frequency f_c using a digitally shaped waveform s(t) of duration T_b . The signal transmitted by the m_t th transmit antenna, $m_t = 1, 2, ..., M_t$, is represented by

$$x_{m_t}(t) = \sqrt{E_t} \sum_{n=0}^{N-1} b(n)s(t - nT_b)e^{j2\pi f_c t} w_{m_t}$$
 (1)

where E_t denotes the transmitted energy per bit per antenna and $w_{m_t} \in \mathbb{C}$ is the complex antenna beam weight parameter. The digitally pulse-coded waveform s(t) is given by $s(t) = \sum_{l=0}^{L-1} s(l) p_{T_c} \left(t - lT_c\right)$ where $s(l) \in \{\pm 1/\sqrt{L}\}$ is the lth code bit of the code vector $\mathbf{s}_{L\times 1}$, and $p_{T_c}(.)$ is a square-root raised cosine (SRRC) pulse with roll-off factor α and duration T_c where $T_b = LT_c$ and the bandwidth of the transmitted signal is $\beta = (1+\alpha)/T_c$. For clarity in the presentation, it is assumed that the individual pulses are normalized to unit energy, $\int_0^{T_c} |p_{Tc}(t)|^2 dt = 1$. The receiver consists of M_T antenna elements. The receiver antenna-front after carrier

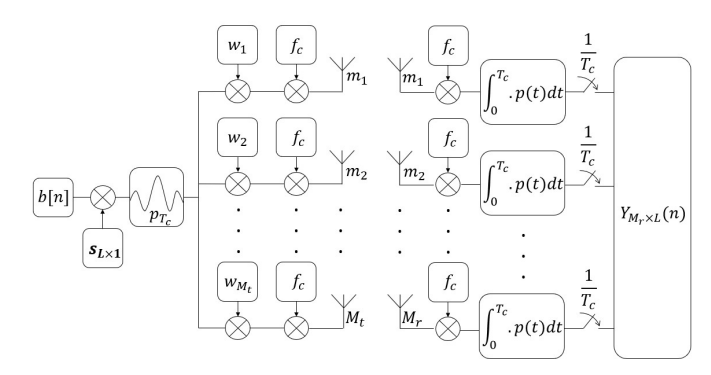


Fig. 1: MIMO system model.

demodulation of the transmitted signal captures

$$\mathbf{r}_{M_r \times 1}(t) = \sqrt{E_t} \sum_{n=0}^{N-1} b(n)s(t - nT_b)\mathbf{H}^T \mathbf{w}_{M_t} + \mathbf{i}(t) + \mathbf{n}(t)$$
(2)

where $\mathbf{H} \in \mathbb{C}^{M_t \times M_r}$ is a generic MIMO channel matrix assumed to remain constant over NT_b sec,

$$\mathbf{H} \triangleq \begin{bmatrix} h_{1,1} & h_{1,2} & \dots & h_{1,M_r} \\ h_{2,1} & h_{2,2} & \dots & h_{2,M_r} \\ \vdots & \vdots & \ddots & \vdots \\ h_{M_t,1} & h_{M_t,2} & \dots & h_{M_t,M_r} \end{bmatrix}, \tag{3}$$

where $h_{m_t,m_r} \in \mathbb{C}$ is the complex coefficient of the channel between the m_t th transmit antenna and the m_r th receive antenna. If two transmit antennas $m_t = i, j$ are in the near field of $m_r = k$, then the phase of $h_{i,k}$ and $h_{j,k}$ vary significantly. Commonly, the beginning of the far field is considered at the distance at which the experienced phase difference is less than $\pi/8$ (Fraunhofer distance). Further on in (2), $\mathbf{w}_{M_t} \in \mathbb{C}^{M_t}$ is the transmitter beam weight vector, $\mathbf{n}(t) \in \mathbb{C}^{M_r imes \mathring{1}}$ denotes a complex Gaussian noise process that is assumed white both in time and space, and $\mathbf{i}(t) \in \mathbb{C}^{M_r}$ models comprehensively environmental disturbance of any other form. For a given fixed bit period n, n = 1, 2, ..., N, upon pulse matched-filtering and sampling over L pulses at each receive antenna element, the collected values are organized in the form of a space-time data matrix $\mathbf{Y}_{M_r \times L}(n)$ (see Fig. 1). The data matrix is then vectorized to

$$\mathbf{y}_{M_rL\times 1}(n) = Vec\{\mathbf{Y}_{M_r\times L}(n)\} =$$

$$= \sqrt{E_t}b(n)(\mathbf{s}\otimes \mathbf{H}^T)\mathbf{w}_{M_t} + \mathbf{i}(n) + \mathbf{n}(n)$$
(4)

where i(n) and n(n) represent post pulse-matched-filtering interference and white noise in the space-time receiver domain.

III. WAVEFORM OPTIMIZATION FUNDAMENTALS

In this section, we derive the maximum-SINR optimal joint space-time receiver filter in the M_rL product vector space and we find its output SINR as a function of s (time-domain code) and \mathbf{w}_{M_t} (transmit beam vector), which creates the foundation for space and time transmit waveform optimization

(interference avoidance). For the given received space-time data vector in (4), the space-time receiver matched filter (MF) is by definition given by

$$\mathbf{w}_{\mathrm{MF}} \triangleq E\left\{\mathbf{y}_{M_rL\times 1}(n)\ b(n)\right\} = (\mathbf{s} \otimes \mathbf{H}^T)\mathbf{w}_{M_t}. \tag{5}$$

The compound space-time disturbance $\mathbf{i}(n) + \mathbf{n}(n)$, assumed to be zero mean for simplicity, has autocorrelation/autocovariance matrix defined by

$$\mathbf{R}_{i+n} \triangleq E\left\{ \left(\mathbf{i}(n) + \mathbf{n}(n) \right) \left(\mathbf{i}(n) + \mathbf{n}(n) \right)^{H} \right\} \in \mathbb{C}^{M_r L \times M_r L}.$$
 (6)

Considering (5) and (6), the space-time maximum SINR receiver filter becomes

$$\mathbf{w}_{\text{max-SINR}} = k \, \mathbf{R}_{i+n}^{-1} (\mathbf{s} \otimes \mathbf{H}^T) \mathbf{w}_{M_t}, \, k \in \mathbb{C}.$$
 (7)

We can now calculate the output SINR of the maximum SINR space-time receiver filter as follows,

$$\mathrm{SINR}(\mathbf{s}, \mathbf{w}_{M_t}) \triangleq \frac{\mathrm{E}\left\{\left|\mathbf{w}_{\mathrm{max-SINR}}^{H}\left(\sqrt{E_t}b(n)(\mathbf{s} \otimes \mathbf{H}^T)\mathbf{w}_{M_t}\right)\right|^2\right\}}{\mathrm{E}\left\{\left|\mathbf{w}_{\mathrm{max-SINR}}^{H}(\mathbf{i}(n) + \mathbf{n}(n))\right|^2\right\}}$$

$$= E_t \left[\mathbf{s} \otimes \mathbf{H}^T \mathbf{w}_{M_t} \right]^H \mathbf{R}_{i+n}^{-1} (\mathbf{s} \otimes \mathbf{H}^T) \mathbf{w}_{M_t}. \tag{8}$$

We see, therefore, that the SINR at the output of the maximum SINR space-time receiver filter for the near-field MIMO link model under examination is a closed form expression of the transmit beam weight vector $\mathbf{w}_{M_t} \in \mathbb{C}^{M_t}$ and the time domain code vector $\mathbf{s} \in \{\pm 1/\sqrt{L}\}^L$. The next step is to investigate what waveform design variables \mathbf{w}_{M_t} and \mathbf{s} maximize the maximum attainable SINR by the receiver filter for a locally sensed space-time disturbance-only autocorrelation matrix

$$\widehat{\mathbf{R}}_{i+n} = \sum_{k=1}^{K} \left(\mathbf{i}(k) + \mathbf{n}(k) \right) \left(\mathbf{i}(k) + \mathbf{n}(k) \right)^{H}$$
(9)

over K samples and estimated MIMO channel state information matrix \mathbf{H} .

IV. SPACE-TIME WAVEFORM DESIGN

In this section, we develop and describe in implementation detail the space-first-time-next waveform design method, i.e., we first suggest an optimized transmit beam weight vector \mathbf{w}_{M_t} and then find the conditionally optimal code vector s given \mathbf{w}_{M_t} . We concentrate first on the space domain operation. Considering only the lth column of the data matrix $\mathbf{Y}_{M_r \times L}(n)$ in Fig. 1 and following the notation in (2), we have

$$\mathbf{y}_l(n) = \sqrt{E_t}b(n)s(l)\mathbf{H}^T\mathbf{w}_{M_t} + \mathbf{i}(l,n) + \mathbf{n}(l,n) \in \mathbb{C}^{M_r},$$
 (10)

 $l \in \{1,2,...,L\}, n \in \{1,2,...,N\}$. The space-only disturbance autocorrelation matrix is defined by

$$\mathbf{R}_{i+n}^{s} \triangleq E\left\{ \left(\mathbf{i}(l,n) + \mathbf{n}(l,n) \right) \left(\mathbf{i}(l,n) + \mathbf{n}(l,n) \right)^{H} \right\} \in \mathbb{C}^{M_r \times M_r}; \quad (11)$$

the space-only maximum SINR filter is

$$\mathbf{w}_{\text{max-SINR}} = k \mathbf{R}_{i+n}^{s^{-1}} \mathbf{H}^T \mathbf{w}_{M_t} \in \mathbb{C}^{M_r}, k \in \mathbb{C};$$
 (12)

and its output SINR is

$$SINR(\mathbf{w}_{M_t}) = E_t \left(\mathbf{H}^T \mathbf{w}_{M_t} \right)^H \mathbf{R}_{i+n}^{s^{-1}} \left(\mathbf{H}^T \mathbf{w}_{M_t} \right). \tag{13}$$

By (13) (a quadratic expression in $\mathbf{H}^T\mathbf{w}_{M_t}$, we recognize that if $\mathbf{q}_{space} \in \mathbb{C}^{M_r}$ is the maximum-eigenvalue eigenvector of the space domain inverse disturbance autocorrelation matrix \mathbf{R}_{i+n}^{s-1} , then the maximum SINR optimal beam weight vector $\mathbf{w}_{M_t}^{opt}$ is such that

$$\mathbf{H}^T \mathbf{w}_{M_{\star}}^{opt} = \mathbf{q}_{space}. \tag{14}$$

If $M_t = M_r$ and $\mathbf{H} \in \mathbb{C}^{(M_t = M_r) \times (M_t = M_r)}$ is full rank, then

$$\mathbf{w}_{M_t}^{opt} = inv(\mathbf{H}^T)\mathbf{q}_{space}.$$
 (15)

If $M_t \neq M_r$ and $\mathbf{H}\mathbf{H}^T$ is full rank (i.e., $M_t < M_r$), then we calculate

$$\mathbf{w}_{M_t}^{opt} = inv(\mathbf{H}\mathbf{H}^T)\mathbf{H}\mathbf{q}_{space}.$$
 (16)

The next step is to search for a binary antipodal code sequence $\mathbf{s} \in \{\pm 1/\sqrt{L}\}^L$ so that the corresponding final spacetime post-filtering SINR $(\mathbf{s}, \mathbf{w}_{M_t}^{opt})$ is maximized. Utilizing (8) for fixed $\mathbf{w}_{M_t} = \mathbf{w}_{M_t}^{opt}$, the remaining optimization problem can be written as

$$\mathbf{s}^{\text{opt}} = \underset{\mathbf{s} \in \{\pm 1/\sqrt{L}\}^L}{\operatorname{argmax}} \left\{ \left[(\mathbf{s} \otimes \mathbf{H}^T) \mathbf{w}_{M_t}^{opt} \right]^H \mathbf{R}_{i+n}^{-1} (\mathbf{s} \otimes \mathbf{H}^T) \mathbf{w}_{M_t}^{opt} \right\}$$
(17)

where $\mathbf{R}_{i+n} \in \mathbb{C}^{M_rL \times M_rL}$ is the joint space-time disturbance autocorreation matrix defined by (6). An optimized code sequence for the given $\mathbf{w}_{M_t}^{opt}$ transmit beam vector can be found by one-dimensional search over 2^L candidate code sequences. The computational complexity of the search is $\mathcal{O}(2^{L-1})$ (the code-vector quadratic optimization problem is sign insensitive). The overall computational complexity is $\mathcal{O}(2M_t^3 + (M_rL)^3 + 4M_tM_rL + 4M_tM_r + 2^{L-1})$. The separately optimized code and transmit beam weight vectors $\mathbf{s}^{opt}, \mathbf{w}_{M_t}^{opt}$ define the interference-avoiding MIMO link waveform. Under the assumption that $\mathbf{s}^{opt}, \mathbf{w}_{M_t}^{opt}$ are made available to the transmitter within the \mathbf{H} and \mathbf{R}_{i+n} channel coherence time, the output SINR of the joint space-time receiver filter is conditionally maximized.

V. SIMULATIONS STUDIES AND COMPARISONS

The effectiveness of the suggested MIMO waveform optimization technique is demonstrated in this section through simulation studies. The evaluation metric is the SINR at the output of the maximum-SINR space-time receiver filter (all schemes under comparison deploy the corresponding optimal max-SINR space-time receiver filter, which coincides with minimum mean-square error optimal space-time equalization.) To account for disturbance effects, we examine different combinations of near-field/far-field and spread-spectrum/non-spread-spectrum interference signals. We evaluate the performance of the proposed waveform in scenarios with both light and dense interference. Specifically, in the light interference case there are $M_r/2$ interfering transmitters of each interference type, while in the dense interference scenario we assume

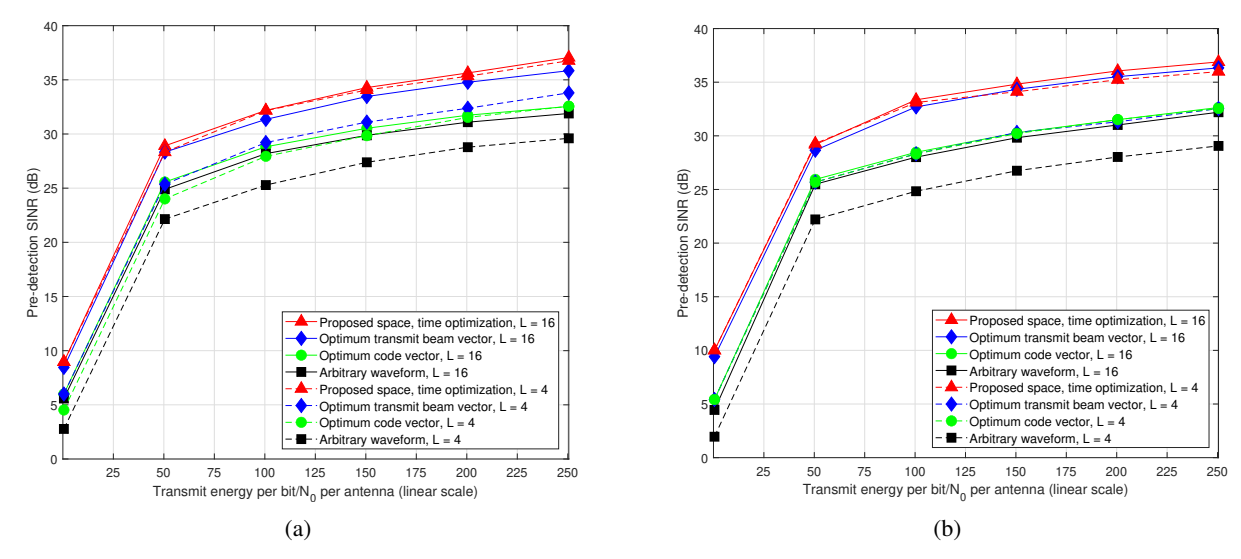


Fig. 2: Pre-detection SINR in near-field non-spread-spectrum interference ($M_t = M_r = M_{i_1} = 4$): (a) Light, (b) dense.

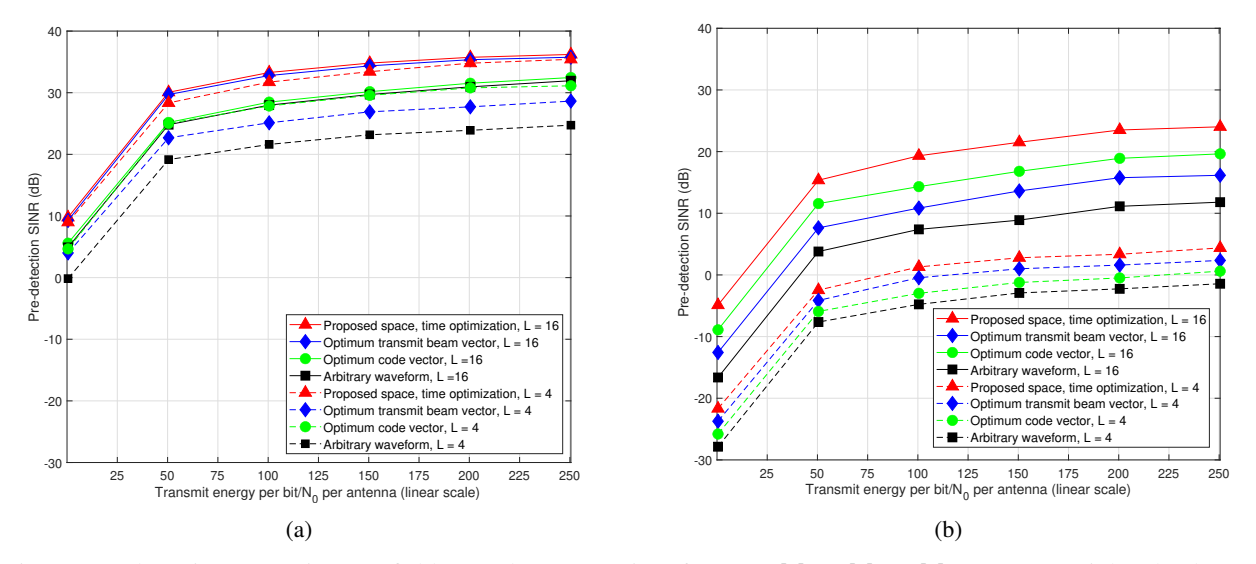


Fig. 3: Pre-detection SINR in near-field spread-spectrum interference ($M_t = M_r = M_{i_3} = 4$): (a) Light, (b) dense.

there are $5M_r$ interfering transmitters of each interference type.

Near-field non-spread-spectrum interfering signals are described by

$$\mathbf{i}_1(t) = \sqrt{E_1} \sum_n b_1[n] p(t - nT_b) \mathbf{H}_1^T \mathbf{w}_{M_{t_1}}$$
 (18)

with bandwidth $\frac{1}{T_b}$, $\mathbf{w}_{M_{t1}}$ transmit antennas, $b_1[n] \in \{\pm 1\}$, and $\mathbf{H}_1 \in \mathbb{C}^{M_{t_1} \times M_r}$. Near-field spread-spectrum interfering signals are described by

$$\mathbf{i}_2(t) = \sqrt{E_2} \sum_n b_2[n] s_2(t - nT_b) \mathbf{H}_2^T \mathbf{w}_{M_{t_2}}$$
 (19)

where $\mathbf{s}_2(t) = \sum_{l=0}^{L-1} \mathbf{s}_2(l) p_{T_c} \left(t - lT_c\right)$, with bandwidth $\frac{L}{T_b}$,

 $\mathbf{s}_2(l) \in \{\pm 1/\sqrt{L}\}, \ \mathbf{w}_{M_{t_2}} \ \text{transmit antennas}, \ b_2[n] \in \{\pm 1\},$ and $\mathbf{H}_2 \in \mathbb{C}^{M_{t_2} \times M_r}.$

Far-field interfering signals have a directional interference effect on the M_r -element receiver front and, for simplicity purposes, we model the array response vector as a linear uniform geometry with inter-element spacing equal to half the carrier wavelength. More specifically, far-field non-spread-spectrum interfering signals are described by

$$\mathbf{i}_3(t) = \sqrt{E_3} \sum_n b_3[n] p(t - nT_b) h_3 \mathbf{a}(\theta_3),$$
 (20)

with bandwidth $\frac{1}{T_b}$, $b_3[n] \in \{\pm 1\}$, flat-fading coefficient $h_3 \in \mathbb{C}$, and array response vector $\mathbf{a}(\theta_3) \in \mathbb{C}^{M_r}$ with angle of arrival $\theta_3 \in (-\frac{\pi}{2}, \frac{\pi}{2})$. Far-field spread-spectrum interfering

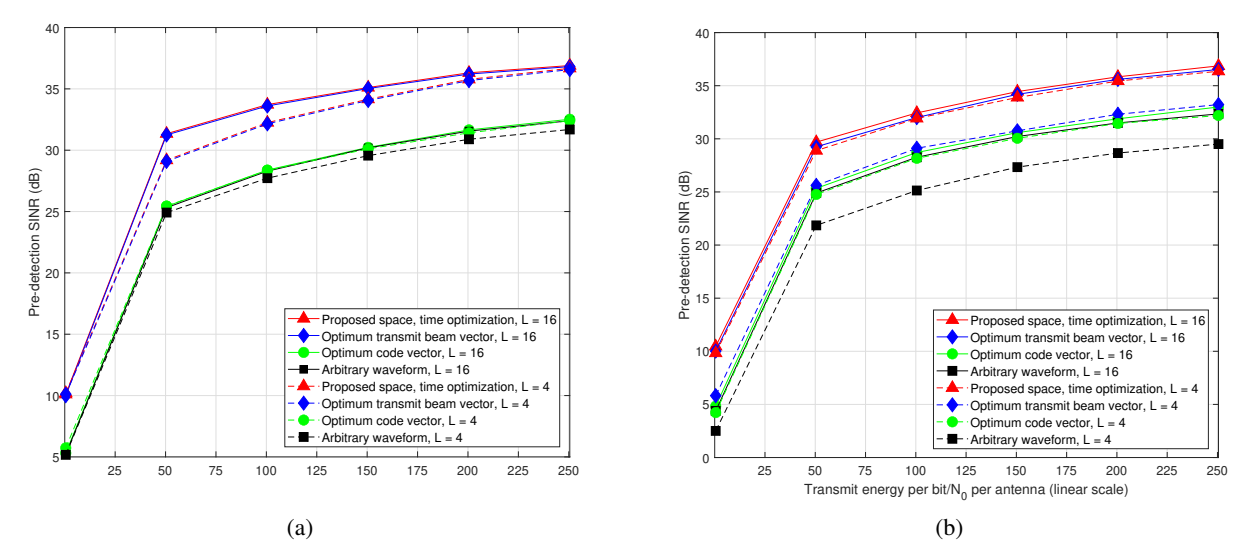


Fig. 4: Pre-detection SINR in far-field non-spread-spectrum interference ($M_t = M_r = M_{i_3} = 4$): (a) Light, (b) dense.

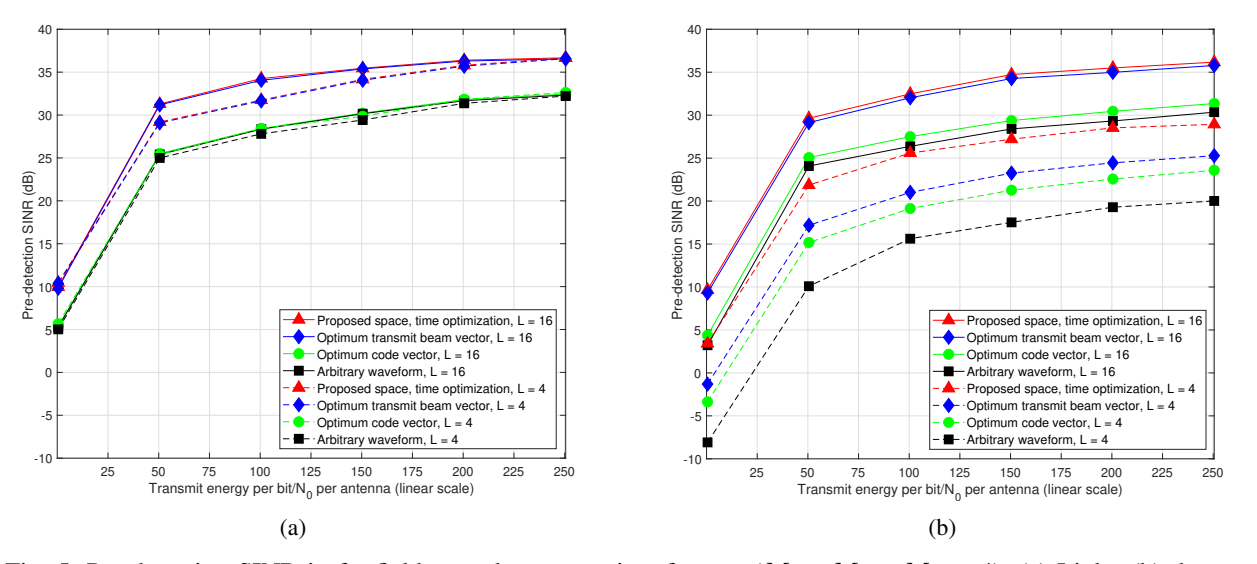


Fig. 5: Pre-detection SINR in far-field spread-spectrum interference ($M_t = M_r = M_{i_4} = 4$): (a) Light, (b) dense.

signals are described by

$$\mathbf{i}_4(t) = \sqrt{E_4} \sum_n b_4[n] s_4(t - nT_b) h_4 \mathbf{a}(\theta_4),$$
 (21)

where $\mathbf{s}_4(t) = \sum_{l=0}^{L-1} \mathbf{s}_4(l) p_{T_c} \, (t-lT_c)$, with bandwidth $\frac{L}{T_b}$, $\mathbf{s}_4(l) \in \{\pm 1/\sqrt{L}\}$, flat-fading coefficient $h_4 \in \mathbb{C}$, and array response vector $\mathbf{a}(\theta_4) \in \mathbb{C}^{M_r}$ with angle of arrival $\theta_4 \in (-\frac{\pi}{2}, \frac{\pi}{2})$.

In Fig. 2, we study the pre-detection SINR of a MIMO link with $M_t=M_r=4$ antennas in near-field non-spread-spectrum interference under no waveform optimization, code only optimization, transmit beam vector only optimization, and proposed transmit beam vector optimization followed by code vector optimization. Fig. 2(a) assumes light interference scenario under codelength L=4 or L=16 where the number

of transmit antennas of each of the $M_r/2=2$ interferers is $M_{i_1}=4$ and their energy-per-bit-over- N_0 value per antenna is set at 10dB where $N_0/2$ denotes the power spectral density of the underlying Gaussian vector noise process assumed to be white across time and space (antenna points). Fig. 2(b) repeats the same studies for dense near-field non-spread-spectrum interference (i.e., $5M_r=20$ interferers) with energy-per-bit-over- N_0 value per antenna equal to 15dB. A broad observation is that the MIMO link easily handles light or dense near-field non-spread-spectrum interference and the proposed waveform optimization approach offers 5dB to 8dB gain (depending on specific scenario and code length) at any transmit-energy-per-bit per antenna level. For example, a target pre-detection SINR value equal to 15dB (practically error-free binary phase-shift-keying decoding) is attained by the proposed space and time

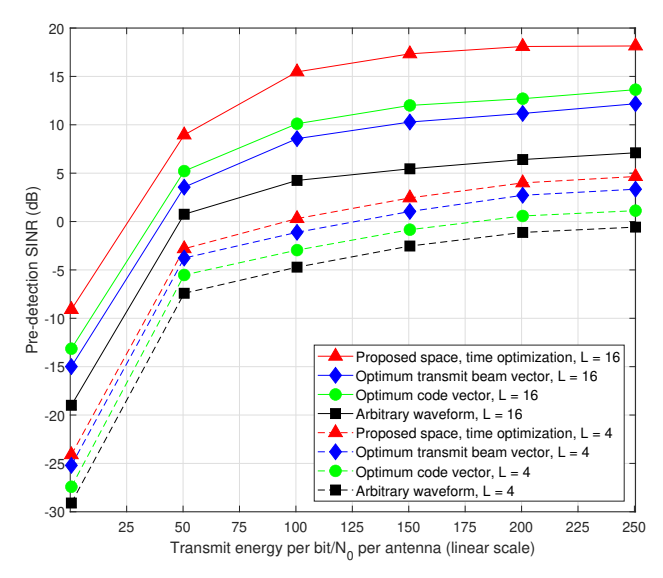


Fig. 6: Pre-detection SINR in dense interference of all types $(M_t = M_r = M_{i_1} = M_{i_2} = M_{i_3} = M_{i_4} = 4)$.

optimization at a 13/35 fraction of the transmit-energy-perbit per antenna comparing against no optimization (arbitrary waveform). As one might expect, for large codelengths, beam vector optimization only and beam vector optimization followed by code vector optimization have about the same predetection SINR yield (Fig. 2(b)).

Fig. 3 repeats the studies of Fig. 2 under the more challenging scenario of spread-spectrum near-field interference with codelengths that match the codelength of the main link. Fig. 3(b), in particular, highlights the difficulty in dealing with dense near-field spread-spectrum disturbance and the importance of having sufficiently large codelength to operate and optimize.

Fig. 4 studies far-field non-spread-spectrum interference with conclusions similar to the near-field corresponding case. Fig. 5 studies spread-spectrum far-field interference, regarded arguably as a simpler case than its near-field counterpart. Indeed, optimized waveforms handle well dense far-field spread-spectrum interference even with small codelengths (Fig. 5(b)).

Finally, Fig. 6 adds up all types of interference in their dense form, that is twenty near-field and twenty far-field non-spread-spectrum interferers, as well as twenty near-field and twenty far-field spread-spectrum interferers, all at 15dB energy-per-bit-over- N_0 value per transmit antenna. Given sufficient degrees of freedom in the time domain, such as L=16, the proposed space-first-time-next optimized MIMO waveform readily attains 10dB or better pre-detection SINR gain.

VI. CONCLUSIONS

We focused on the challenge of creating a dynamic MIMO wireless link over a fixed frequency band that can avoid heavy interference. Given a running local estimate of the disturbance autocorrelation matrix and the MIMO channel

matrix coefficients, we proposed an algorithmic solution that carries out optimal transmit beam weight vector (space-first) and pulse code sequence (time-next) design that maximizes the output SINR of the maximum-SINR joint space-time receiver filter. Extensive simulations studies evaluated the effectiveness of the proposed optimum waveform in the presence of near-field/far-field, spread-spectrum/non-spread spectrum interference, in both light and dense interference scenarios. The studies highlighted the ability of the optimized waveform to maintain "clean" communications in extreme mixed-interference environments.

REFERENCES

- [1] M. U. A. Siddiqui, F. Qamar, F. Ahmed, Q. N. Nguyen, and R. Hassan, "Interference management in 5G and beyond network: Requirements, challenges and future directions," *IEEE Access*, vol. 9, pp. 68 932– 68 965, Apr. 2021.
- [2] S. Naderi, D. B. d. Costa, and H. Arslan, "Channel randomness-based adaptive cyclic prefix selection for secure ofdm system," *IEEE Wireless Comm. Letters*, vol. 11, pp. 1220–1224, June 2022.
- [3] S. Naderi, D. B. da Costa, and H. Arslan, "Joint random subcarrier selection and channel-based artificial signal design aided PLS," *IEEE Wireless Comm. Letters*, vol. 9, pp. 976–980, July 2020.
- [4] H. Salman, S. Naderi, and H. Arslan, "Channel-dependent code allocation for downlink mc-cdma system aided physical layer security," in *Proc. IEEE VTC*, Helsinki, Finland, June 2022, pp. 1–5.
- [5] S. Das and H. Viswanathan, "Interference mitigation through interference avoidance," in *Proc. IEEE Asilomar Conf. on Signals, Syst, and Comp.*, Pacific Grove, CA, Oct. 2006, pp. 1815–1819.
- [6] C. Rose, S. Ulukus, and R. Yates, "Wireless systems and interference avoidance," *IEEE Trans. Wireless Comm.*, vol. 1, pp. 415–428, July 2002.
- [7] K. Tountas, G. Sklivanitis, D. A. Pados, and S. N. Batalama, "All-spectrum digital waveform design via bit flipping," in *Proc. IEEE GLOBECOM*, Abu Dhabi, UAE, Dec. 2018, pp. 1–6.
- [8] G. Sklivanitis, P. P. Markopoulos, S. N. Batalama, and D. A. Pados, "Sparse waveform design for all-spectrum channelization," in *Proc. IEEE ICASSP*, New Orleans, LA, Mar. 2017, pp. 3764–3768.
- [9] G. Sklivanitis, A. Gannon, K. Tountas, D. A. Pados, S. N. Batalama, S. Reichhart, M. Medley, N. Thawdar, U. Lee, J. D. Matyjas, S. Pudlewski, A. Drozd, A. Amanna, F. Latus, Z. Goldsmith, and D. Diaz, "Airborne cognitive networking: design, development, and deployment," *IEEE Access*, vol. 6, pp. 47217–47239, July 2018.
- [10] K. Tountas, G. Sklivanitis, and D. A. Pados, "Directional space-time waveform design for interference-avoiding MIMO configurations," in *Proc. iWAT*, Miami, FL, Mar. 2019, pp. 235–238.
- [11] K. Tountas, G. Sklivanitis, and D. A. Pados, "Dynamic joint PHY-MAC waveform design for IoT connectivity," in *Proc. IEEE ICASSP*, Brighton, UK, May 2019, pp. 8399–8403.
- [12] J. Molins-Benlliure, E. Antonino-Daviu, M. Cabedo-Fabrés, and M. Ferrando-Bataller, "Design of a MIMO 5G indoor base station antenna using unit cells," in *Proc. EuCAP*, Madrid, Spain, Mar. 2022, pp. 1–4.
- [13] J. Zhang, E. Björnson, M. Matthaiou, D. W. K. Ng, H. Yang, and D. J. Love, "Prospective multiple antenna technologies for beyond 5G," *IEEE Journal Select. Areas Comm.*, vol. 38, pp. 1637–1660, Aug. 2020.
- [14] S. Mazokha, S. Naderi, G. I. Orfanidis, G. Sklivanitis, D. A. Pados, and J. O. Hallstrom, "Single-sample direction-of-arrival estimation for fast and robust 3D localization with real measurements from a massive mimo system," in *Proc. IEEE ICASSP*, Rhodes Island, Greece, June 2023, pp. 1–5.
- [15] Y. Takano, H.-J. Su, Y. Shiraishi, and M. Morii, "A spatial-temporal subspace-based compressive channel estimation technique in unknown interference MIMO channels," *IEEE Trans. Signal Proc.*, vol. 68, pp. 300–313, Dec. 2020.
- [16] R. A. Osman, S. N. Saleh, and Y. N. M. Saleh, "A novel interference avoidance based on a distributed deep learning model for 5G-enabled IoT," Sensors, vol. 21, pp. 1–23, Sept. 2021.